

■

,

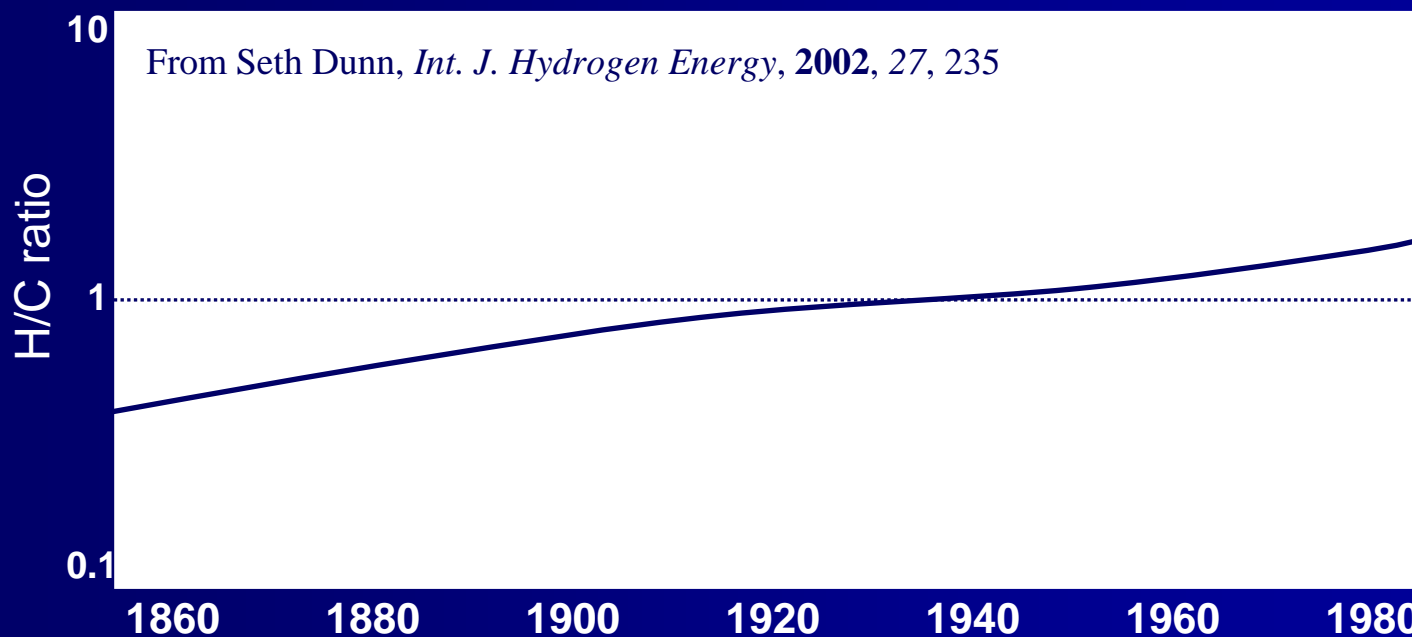
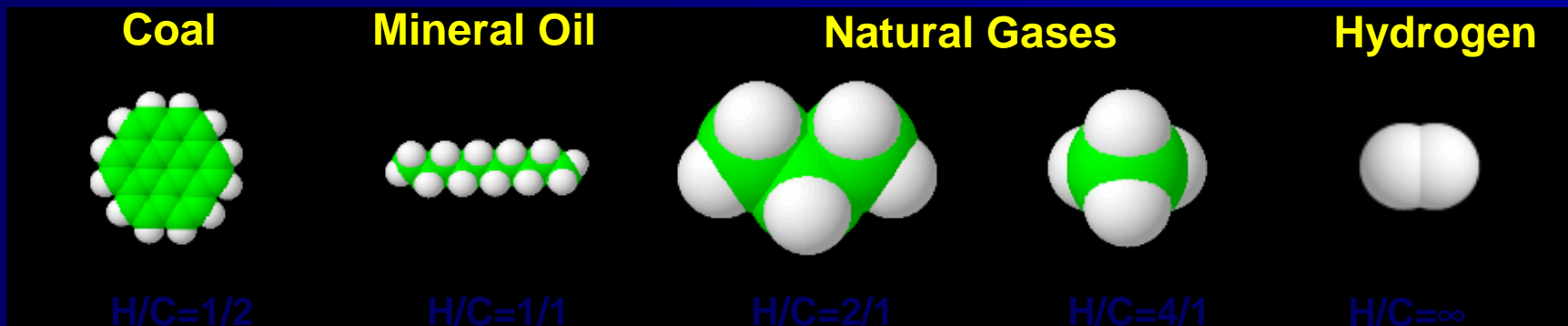
,

,

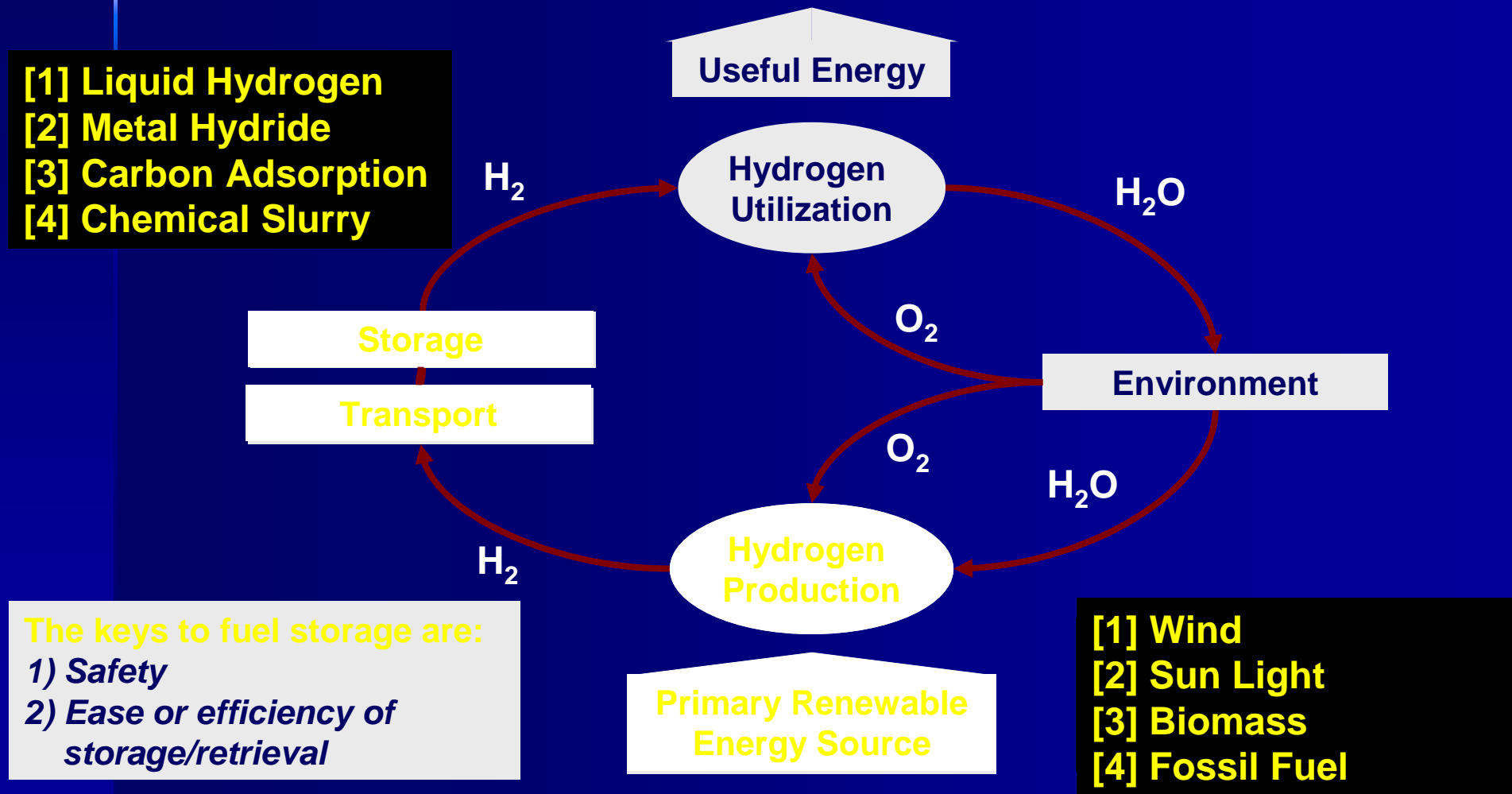
,

,

Change of H:C ratio

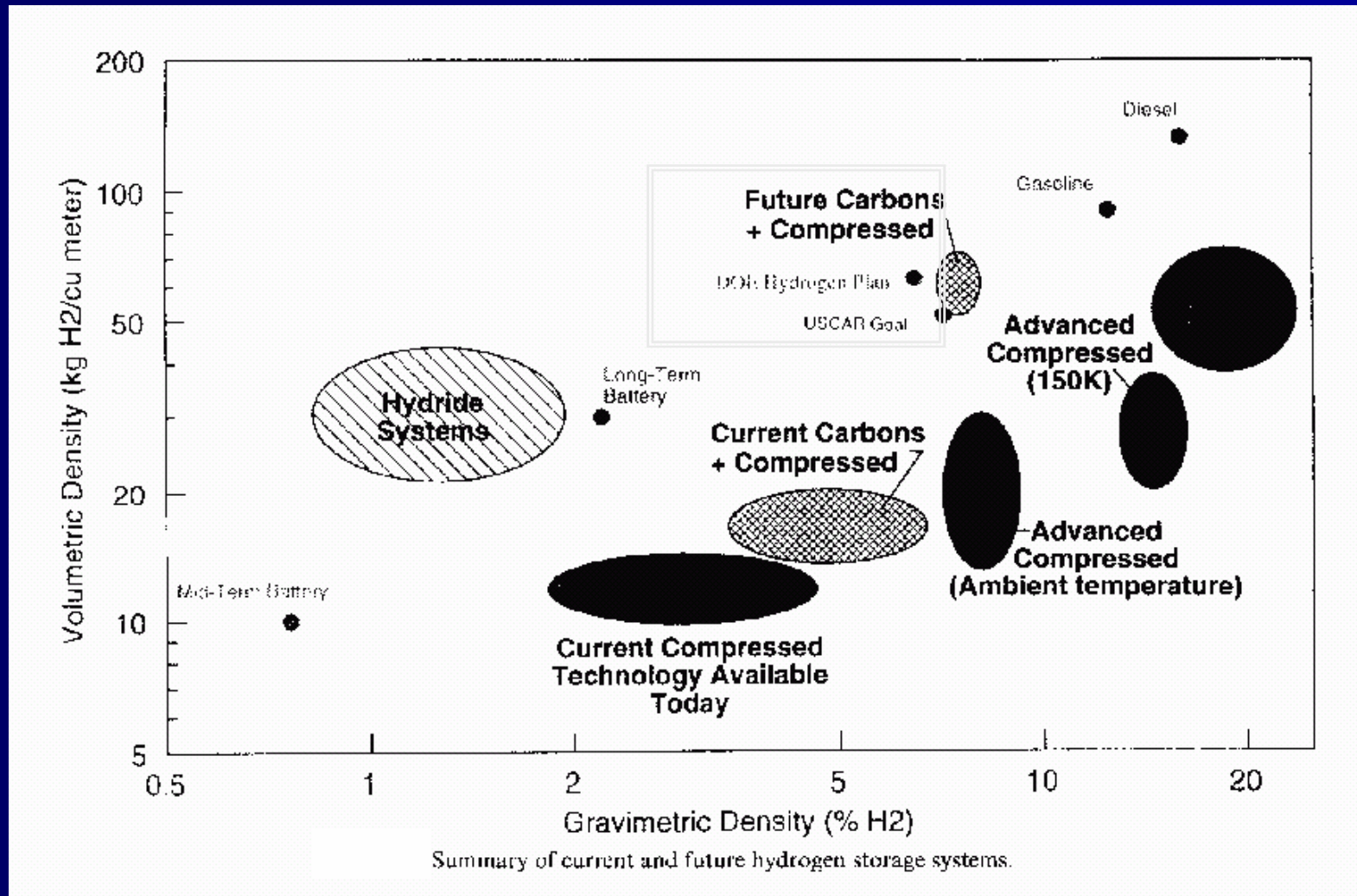


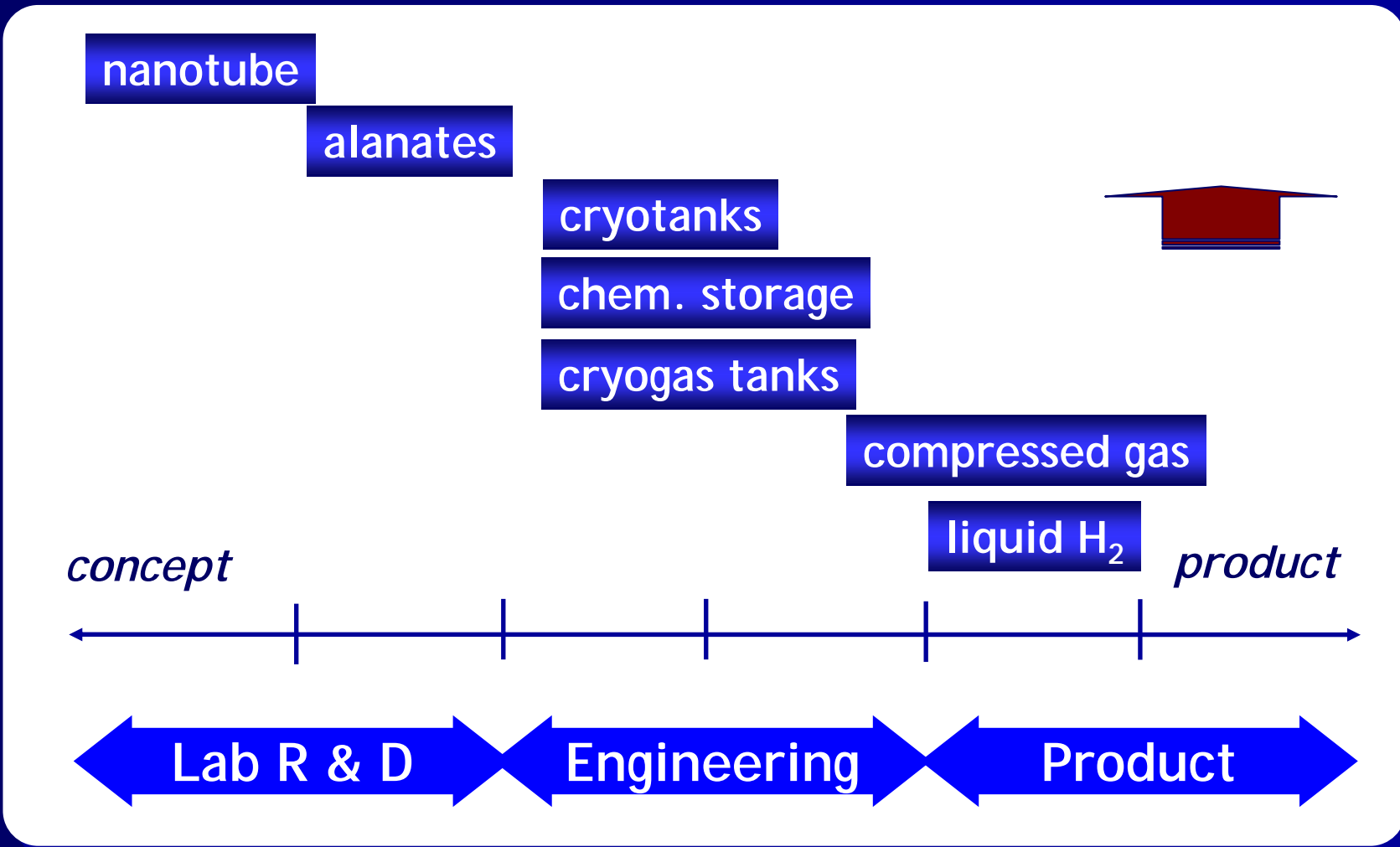
Hydrogen Life Cycle



Hydrogen Storage System - Current and Future

Hynek et al. *Int. J. hydrogen Energy*, 22, 601 (1997)

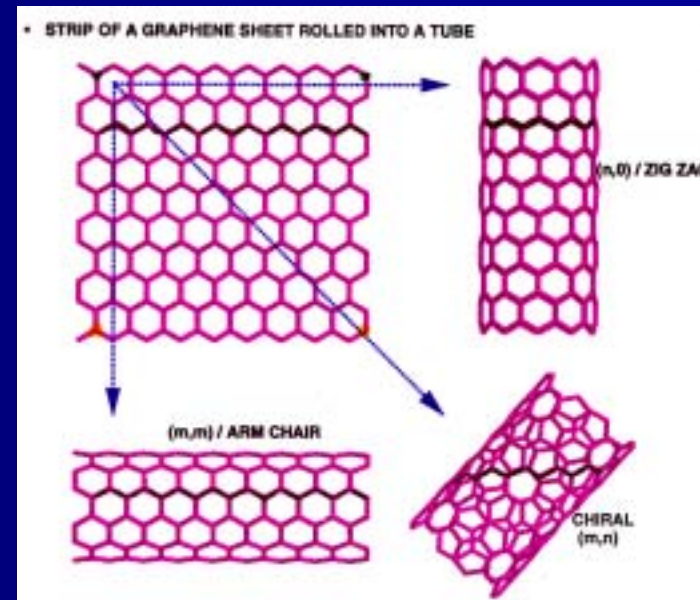
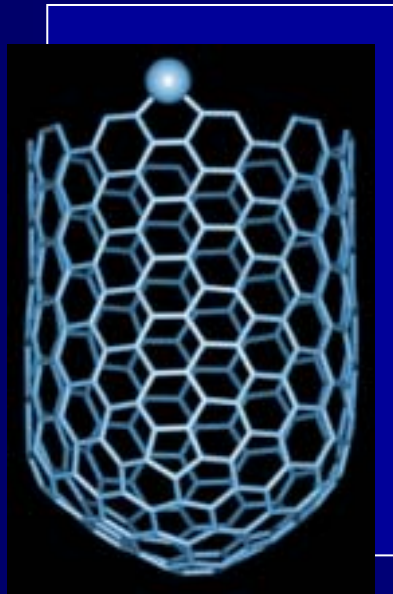




- [1] Microporous carbon
- [2] Metal incorporated nanoporous carbon
- [3] Metal organic framework
- [4] Conducting polymer

Atomic Structure and Electronic Properties of SWNT

Odom et al., *Nature* **391**, 62 (1998).



- Diameter and helicity of defect-free SWNT characterized by

$$\mathbf{c}_h = n\mathbf{a}_1 + m\mathbf{a}_2 \equiv (n, m)$$

- Electronic band structure calculations: metallic when $n/3$ is an integer or $(n, n+3q)$ where q is an integer, and otherwise semiconductors

Metal-like Properties of SWNT

Electronic structure of SWNT by NMR

Tang et al., *Science* **288**, 492 (2000).

- Presence of metallic tube was identified from the measurement of spin-lattice relaxation rates.

Metallic behavior of boron containing-NT by ESR

Hsu et al., *Chemical Physics Letters* **323**, 572 (2000).

Energy Gaps in "Metallic" Single-Walled Carbon Nanotubes

Ouyang et al., *Science* **292**, 702 (2001)

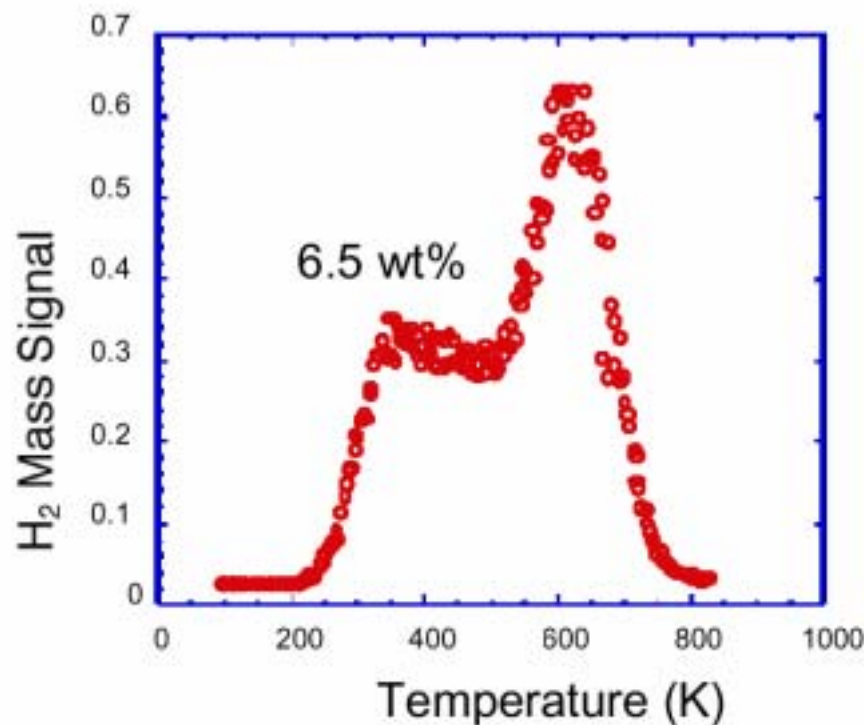
Chemisorption like hydrogen storage in carbon nanotube

or

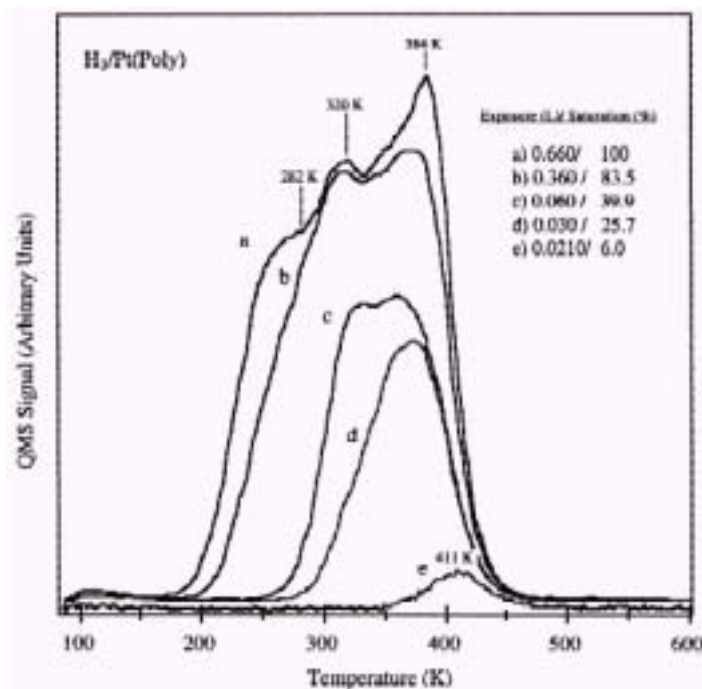
Midway between Van der Waals interaction and chemical bond formation

(~ $19.6 \text{ kJ}\cdot\text{mol}^{-1}$ for binding energy in opened SWNTs, *Nature*, **386**, 377 (1997))

Temperature Programmed Desorption of Hydrogen

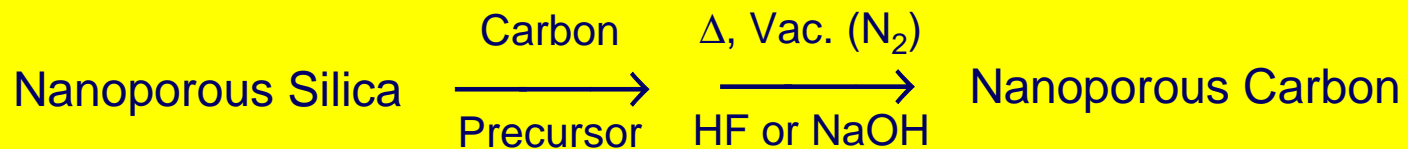
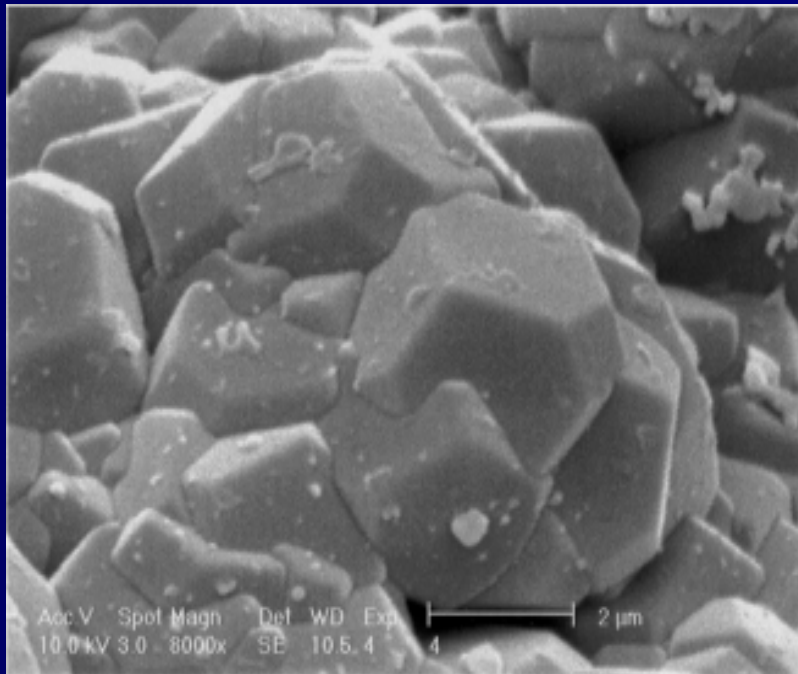


Hydrogen TPD spectrum of degassed sample following a room temperature exposure to 500 torr (From Proceedings of hydrogen program review NREL/CP-570-28890)

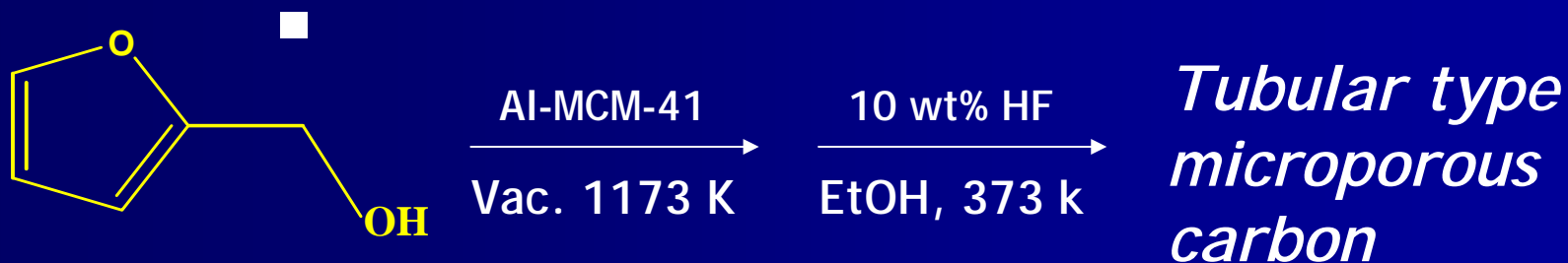


Hydrogen TPD spectrum from polycrystalline Pt taken from Thomas et al.

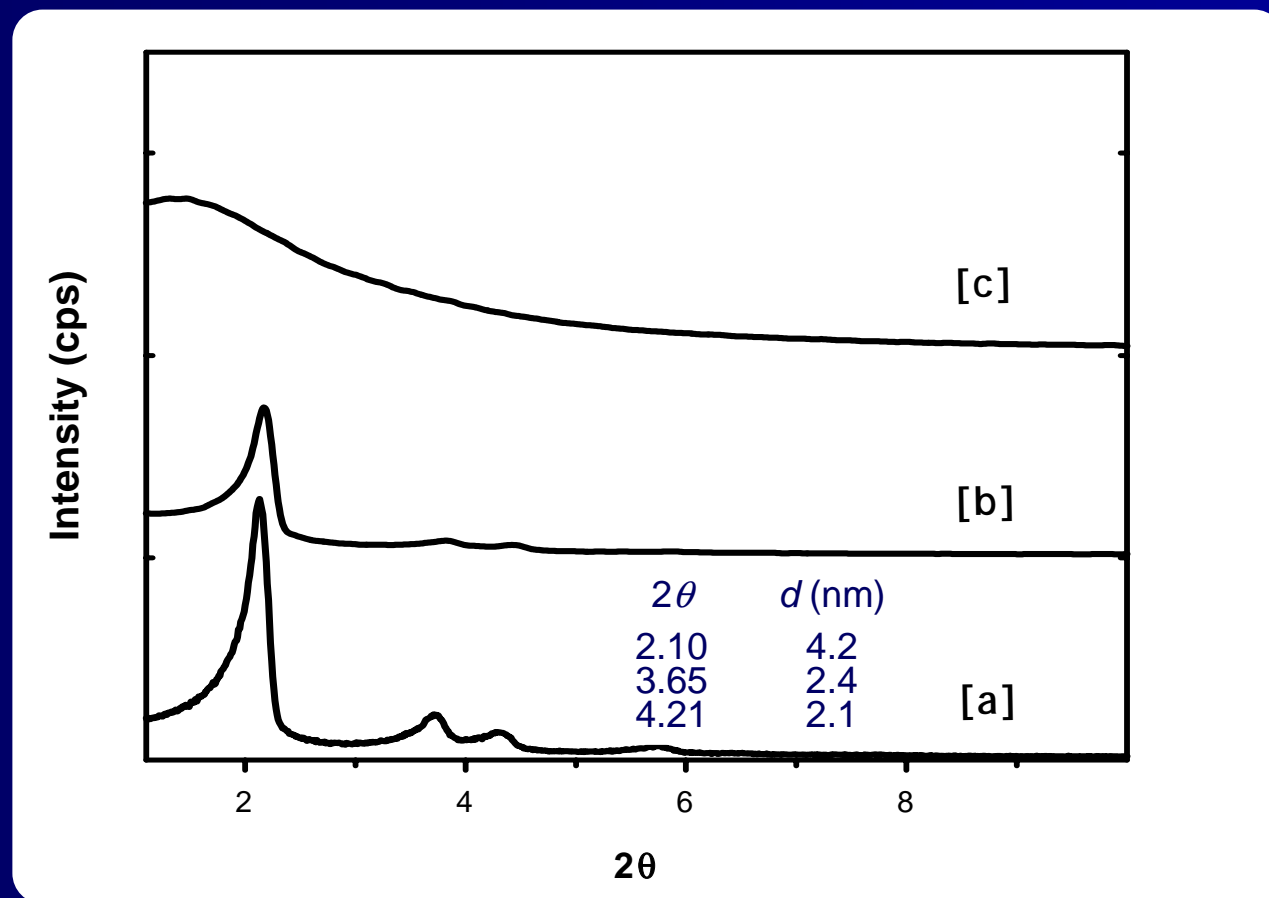
Nanoporous silica and its carbon replica



Carbonization of Furfuryl Alcohol Inside the Channel of the Al-grafted MCM-41



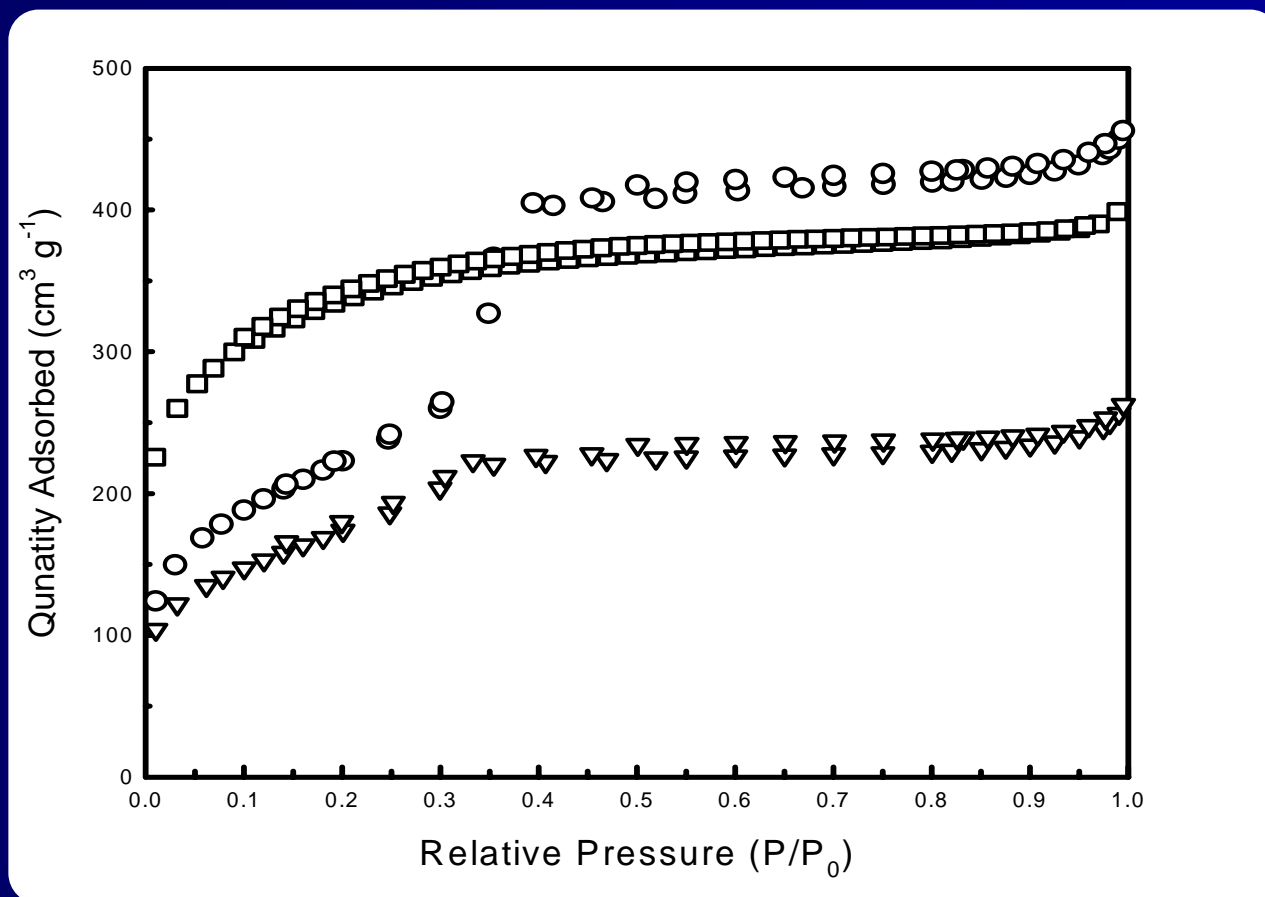
X-ray Diffraction Patterns during the Carbonization



X-ray diffraction patterns of (a) the Al-grafted MCM-41 (Si/Al=10.8), (b) the C/Al-grafted MCM-41 after the carbonization at 1173 K under vacuum and (c) the resulting carbon after the removal of SiO_2 .

Clean Energy Technology Laboratory, Chonnam National University

Change of N₂ Adsorption-desorption Isotherm during the Carbonization



N₂ adsorption-desorption isotherm at 77 K on (○) the Al-grafted MCM-41 (Si/Al=10.8), (▽) the C/Al-grafted MCM-41 after the carbonization at 1173 K under vacuum and (□) the resulting carbon after the removal of SiO₂.

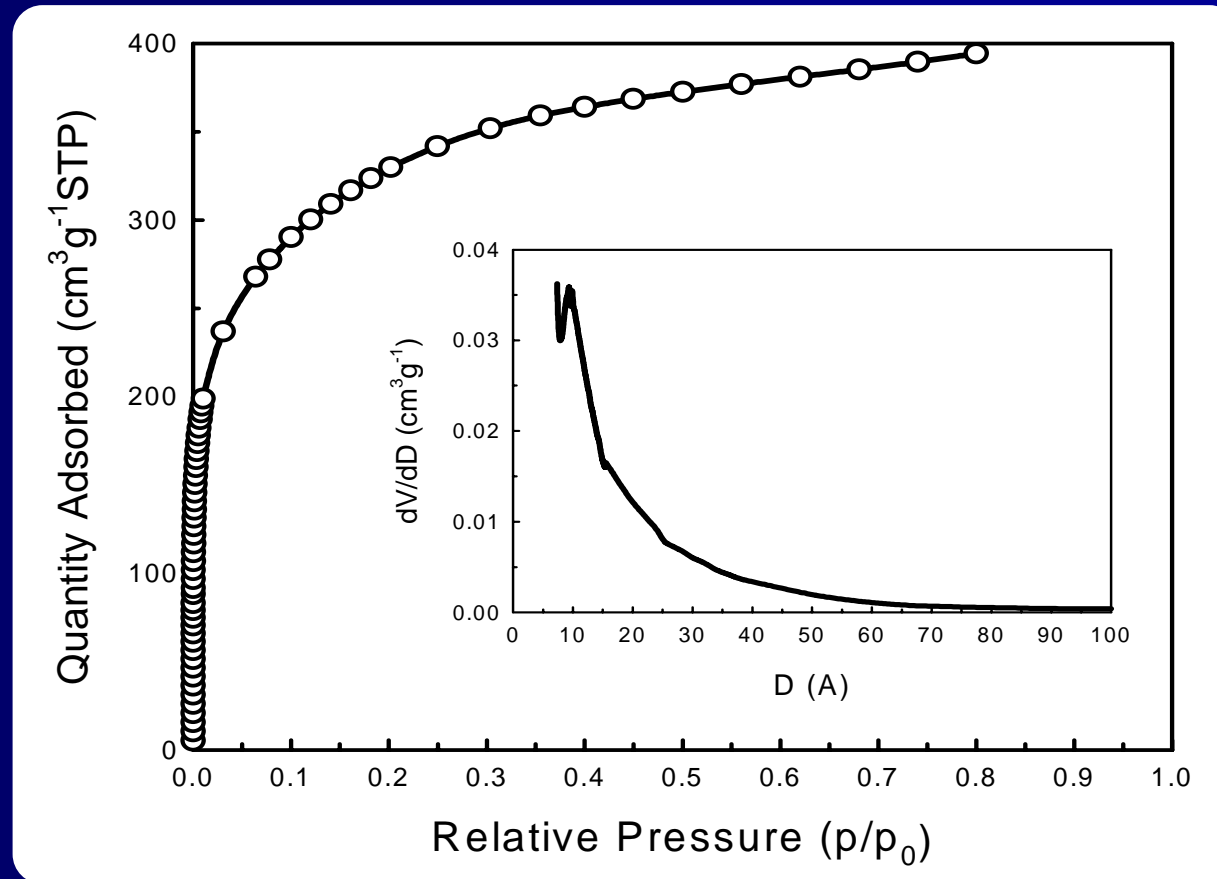
Clean Energy Technology Laboratory, Chonnam National University

Surface Properties of the Sample at the Each Stage of Preparation

sample	S_{BET} (m^2g^{-1})	t -plot		pore size, 4V/A (nm)
		S_{micro} (m^2g^{-1})	S_{meso} (m^2g^{-1})	
Al-MCM-41 (Si/Al=10.8)	809	32	777	3.4
C/Al-MCM-41 Before HF treatment	627	29	599	2.6
Carbon After HF treatment	1137	541	596	2.0

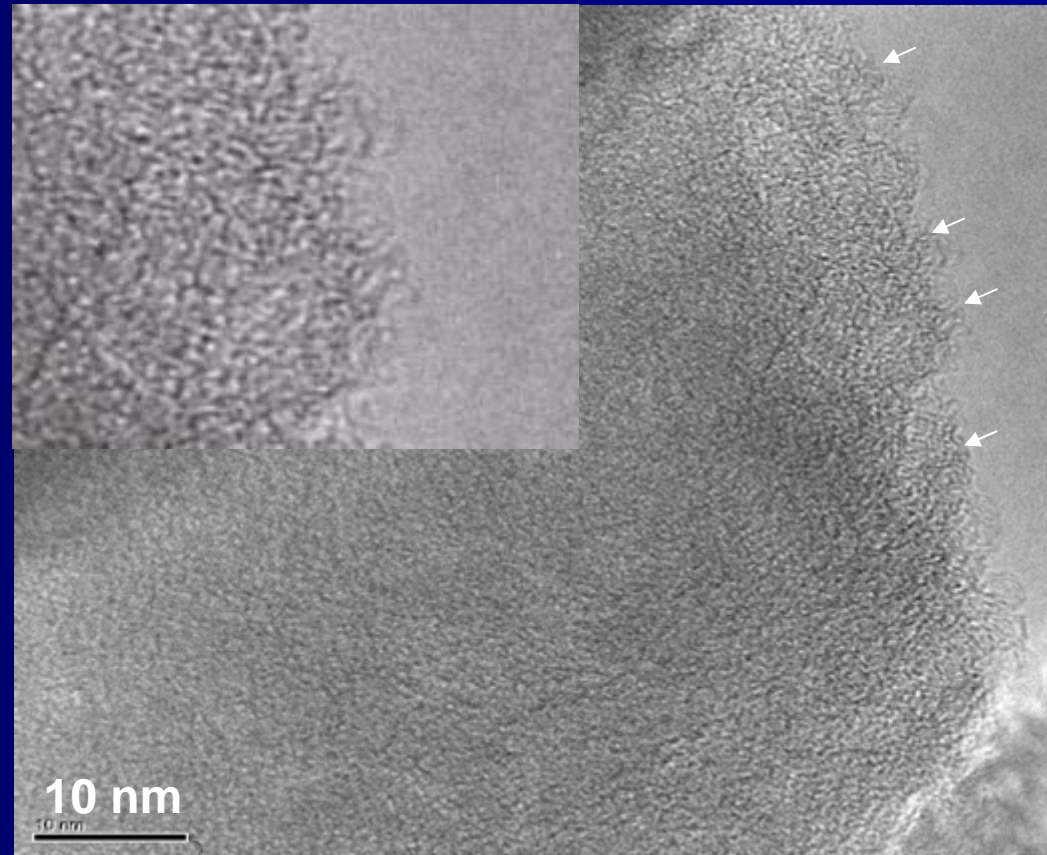
- Significant portion of the pore of the MCM-41 was filled with the polymerized furfuryl alcohol.

Ar Adsorption Isotherm on the Microporous Carbon Obtained from Al-grafted MCM-41 at 89 K



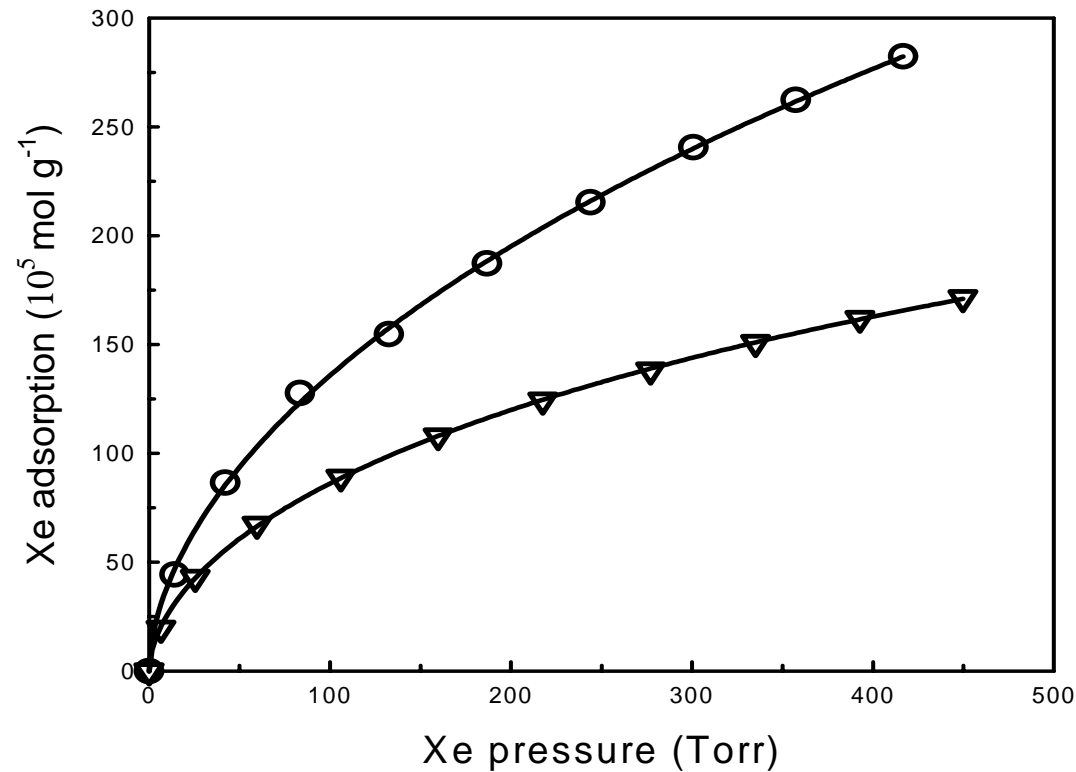
Ar adsorption isotherm on the microporous carbon derived from the Al-grafted MCM-41 (Si/Al=10.8) at 89 K. The inset shows the pore size distribution obtained from the Horvath-Kawazoe method.

Transmission Electron Micrograph of the Tubular Microporous Carbon



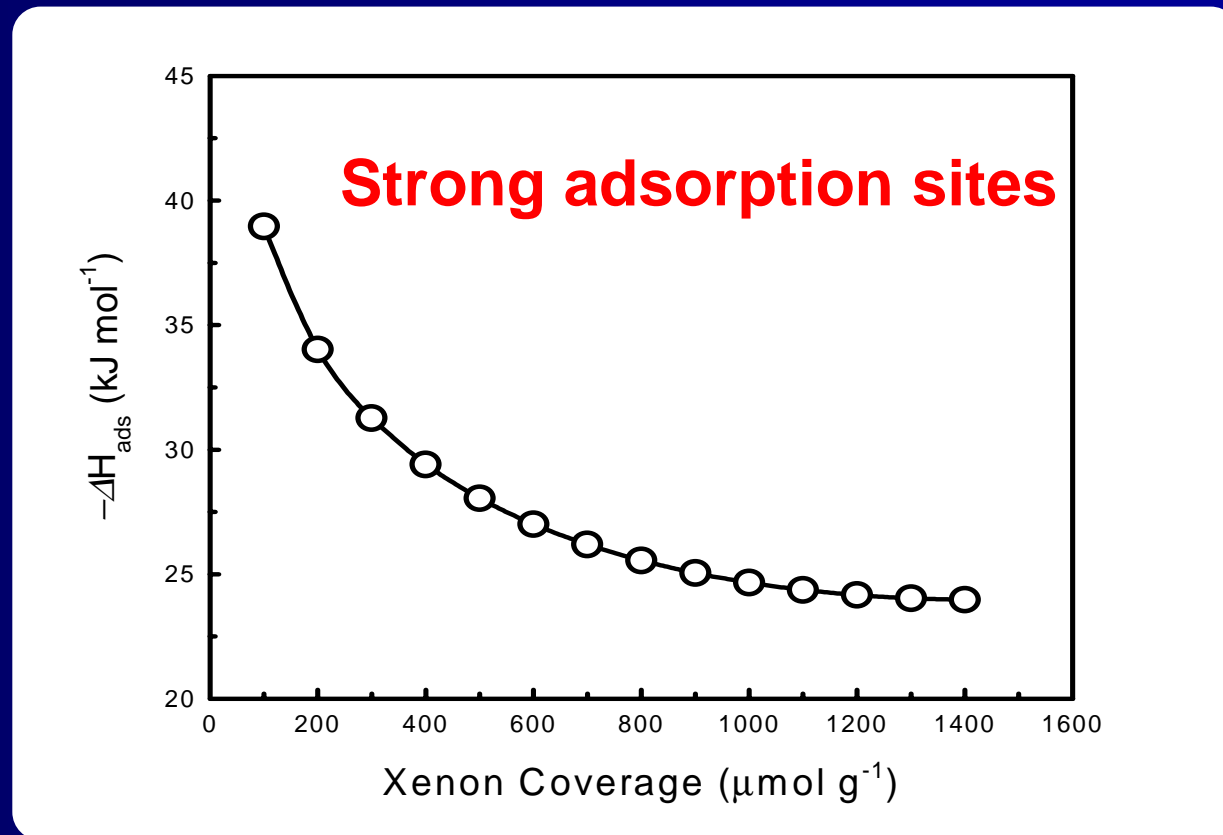
Transmission electron micrograph of the carbon derived from the Al-grafted MCM-41 (Si/Al=10.8) after the removal of SiO_2 .

Xenon Adsorption Isotherm on the Tubular Microporous Carbon



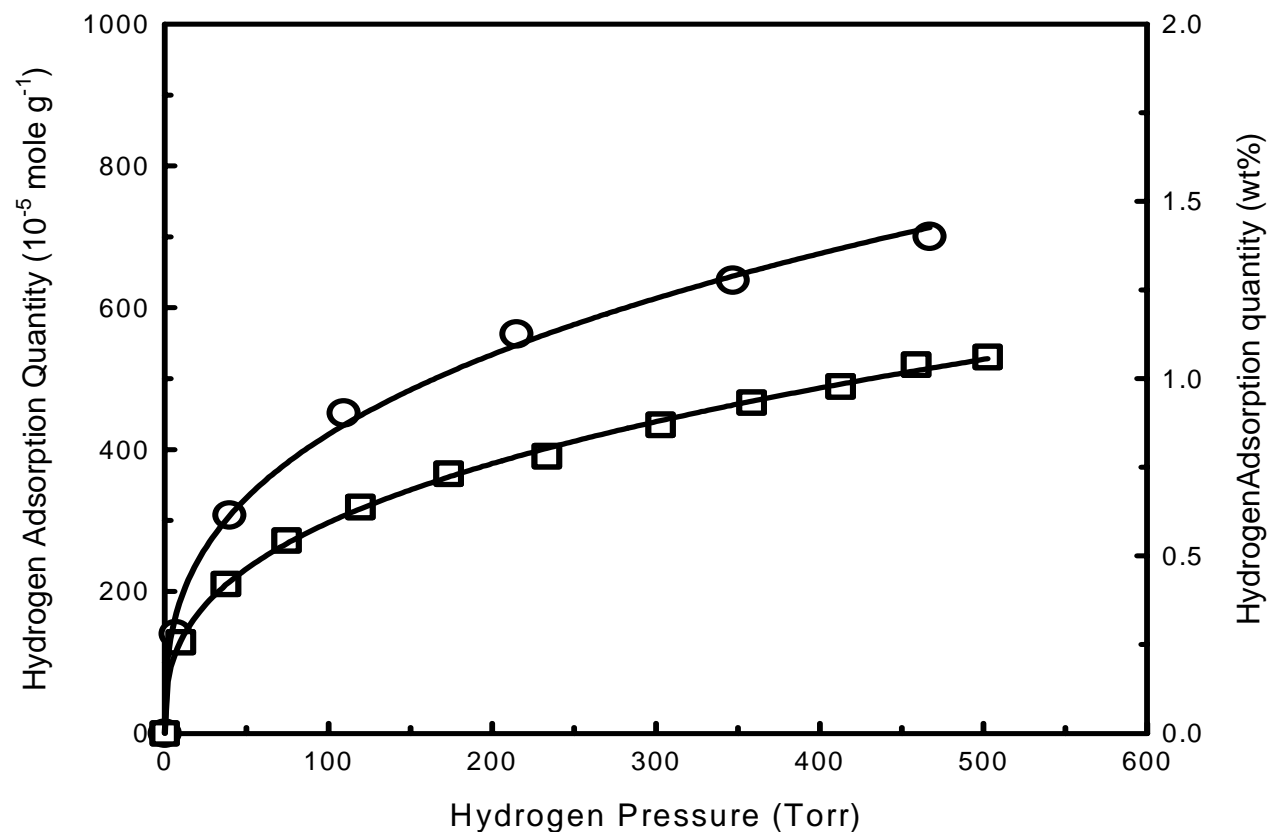
Xenon adsorption isotherms on () tubular microporous carbon and () CMK-1 at 298 K.

Heat of Adsorption of Xenon on the Tubular Microporous Carbon



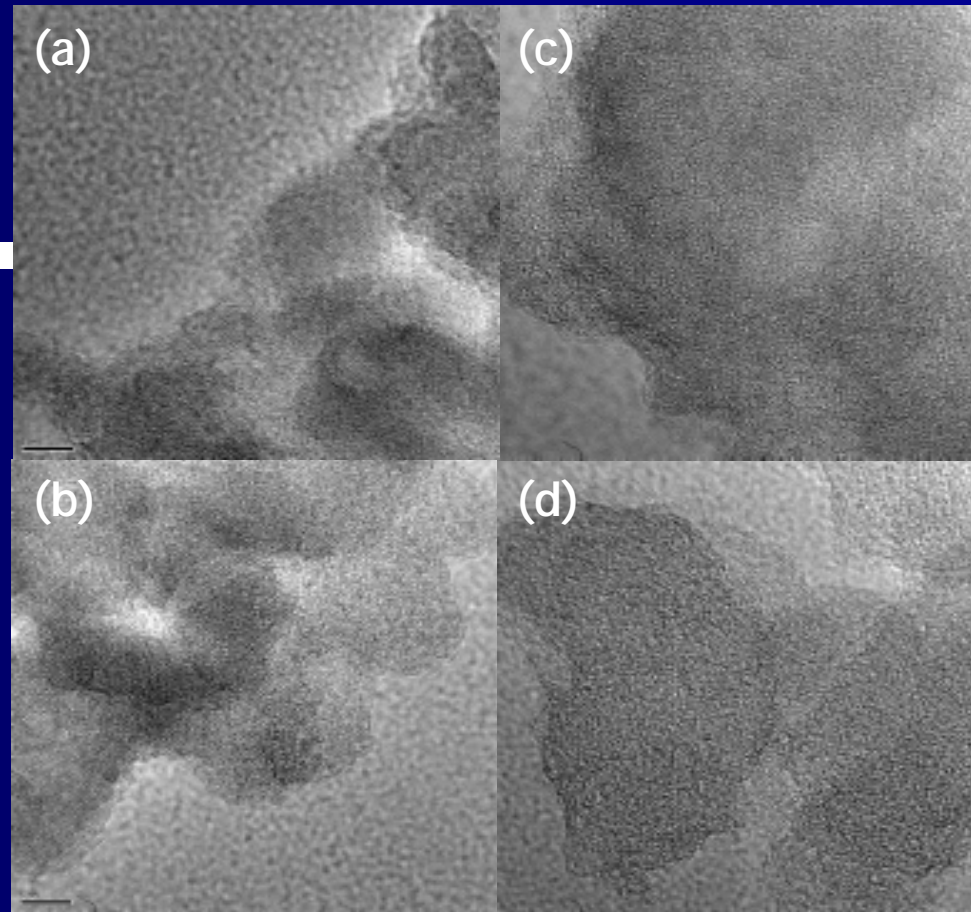
Heat of adsorption of xenon on the microporous tubular carbon at 298 K from the Clausius-Clapeyron equation plotted against the xenon coverage. The three xenon adsorption isotherms were measured at 295 K, 298 K and 301 K, respectively.

Hydrogen Adsorption Isotherm on the Tubular Microporous Carbon



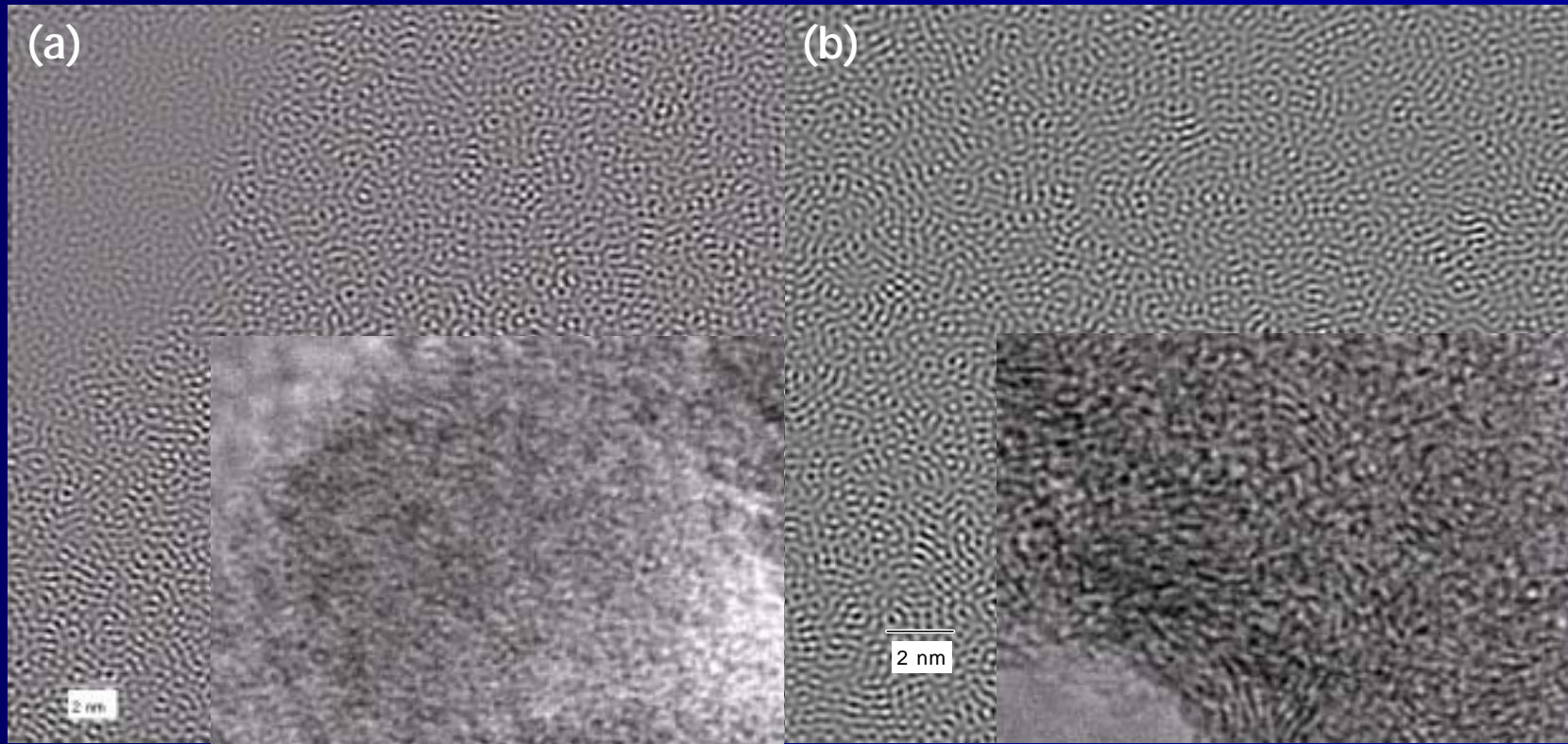
Hydrogen adsorption isotherms on () tubular microporous carbon and () CMK-1 at 77 K.

Transmission Electron Micrograph of the Microporous Carbon from BEA Zeolite



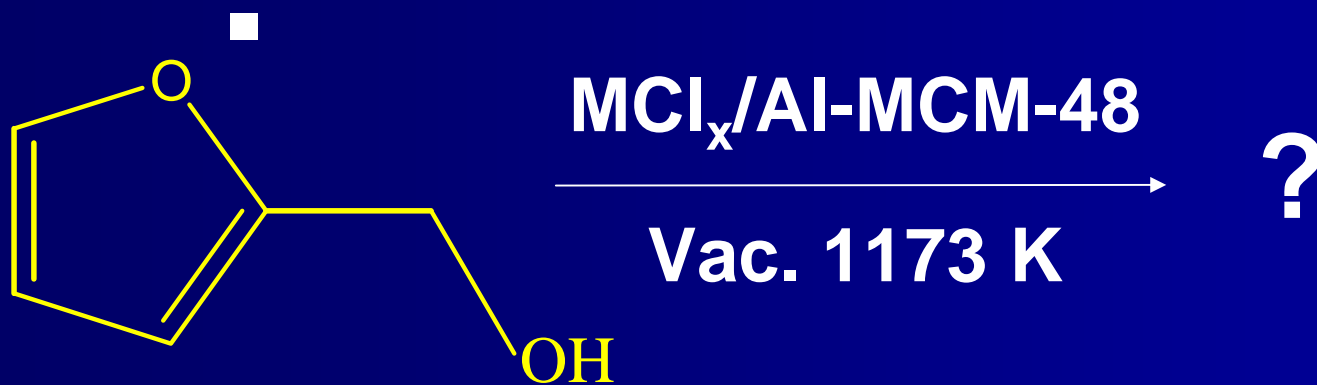
HRTEM micrographs of (a,b) zeolite BEA and (c,d) the microporous carbons after the removal of the zeolite BEA in carbon/silica composites.

Channel Imaging BEA Zeolite and the Microporous Carbon

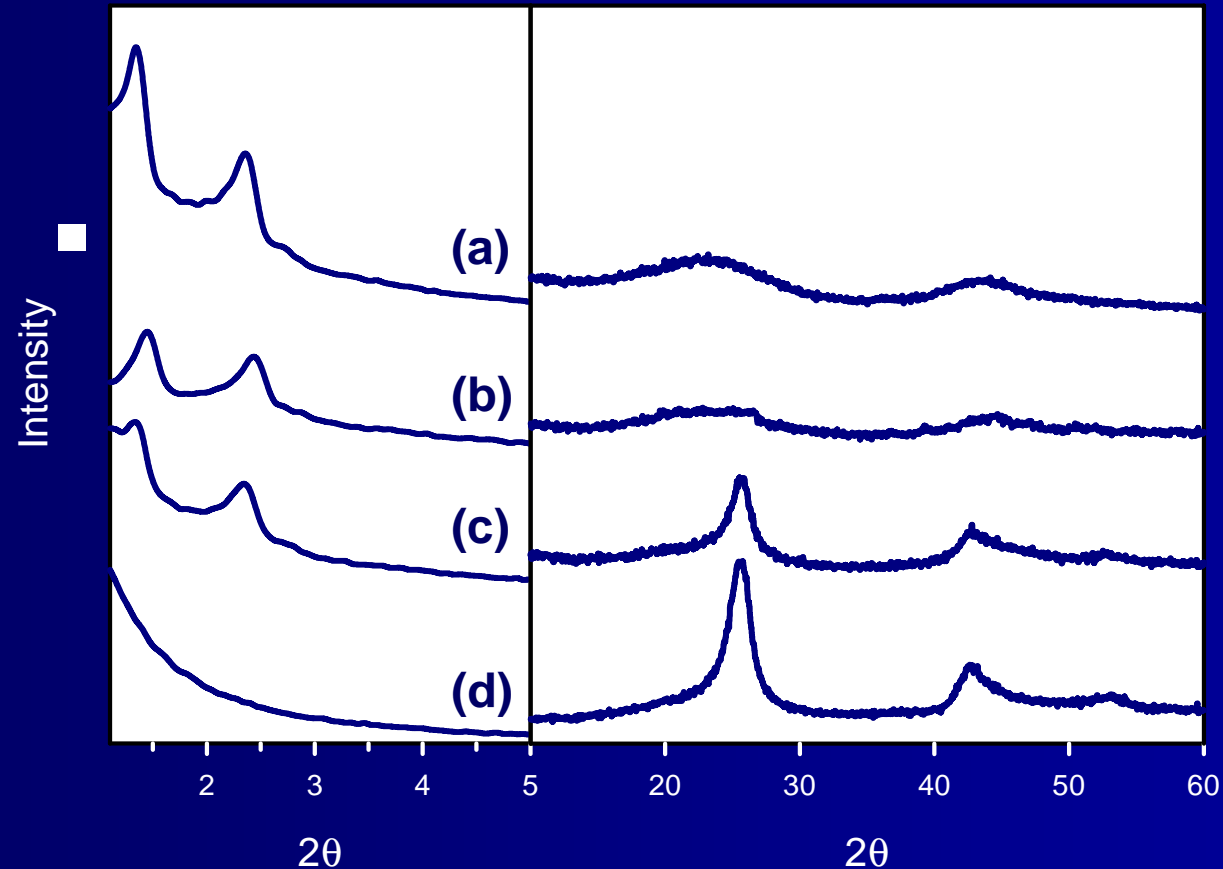


HRTEM micrographs of (a) zeolite BEA and (b) the microporous carbons after the removal of the zeolite BEA in carbon/silica composites. The images were processed through the FFT algorithm implemented GATAN software package.

Synthesis Strategy for Nanoporous Metal-Carbon

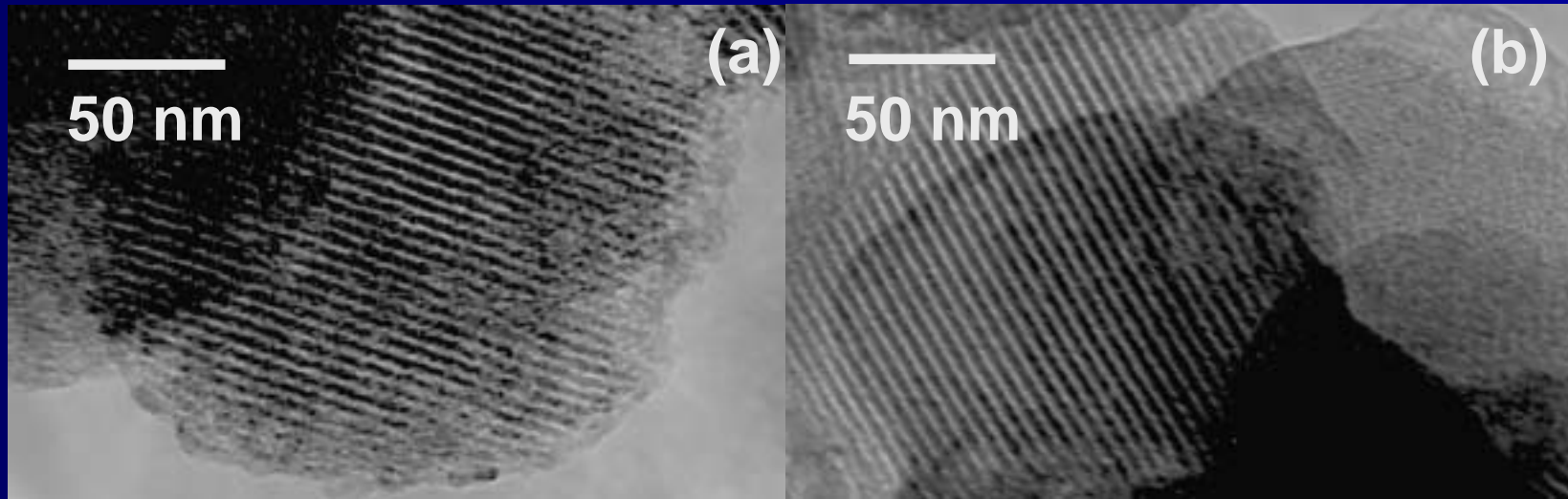


Effect of Metal on the Formation of Nanoporous Carbon



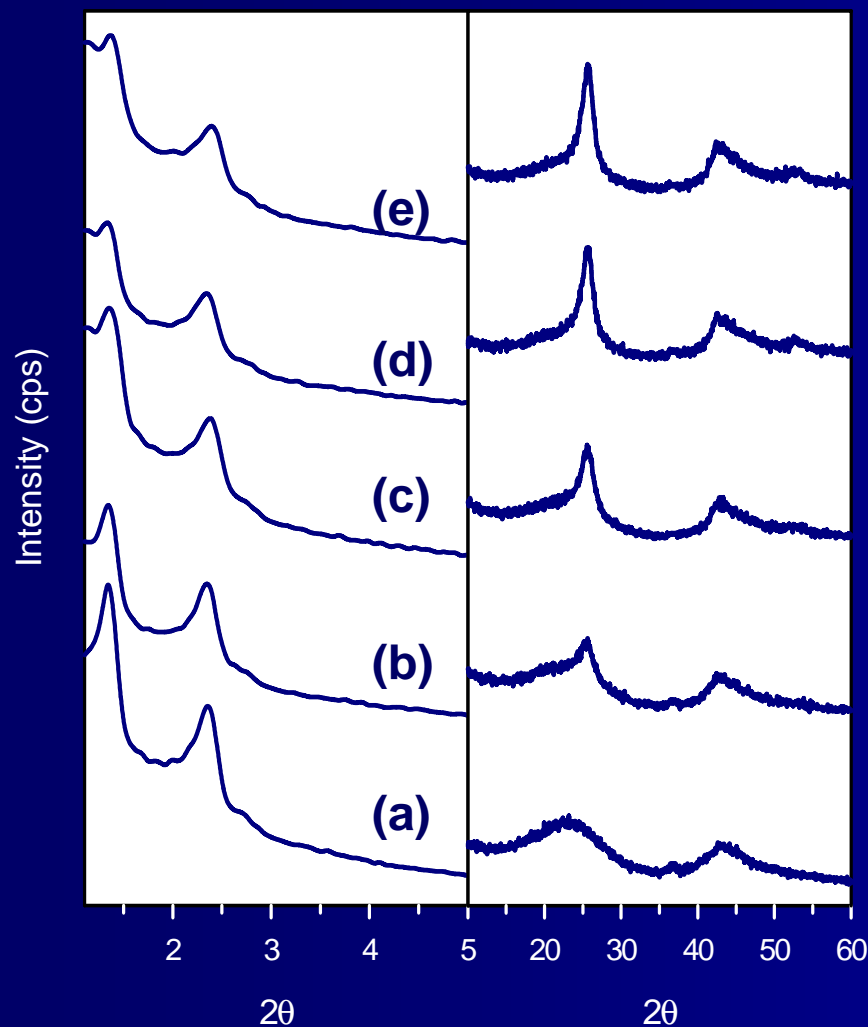
X-ray diffraction patterns of (a) CMK-1, (b) Ni-, (c) Co- and (d) Fe-catalyzed nanoporous carbon. The amount of catalyzing metal was controlled to 10 wt% of the product C content.

Transmission Electron Micrographs of Nanoporous Carbon



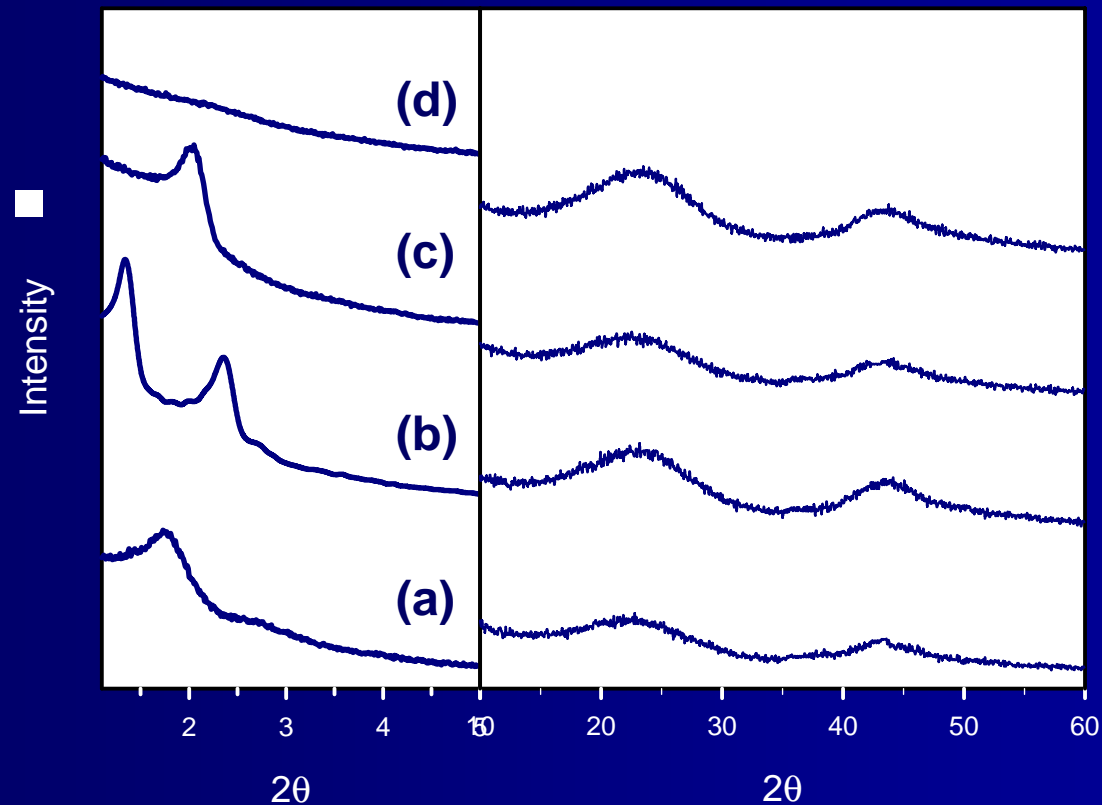
High resolution transmission electron micrographs of (a) CMK-1 and (b) *g*-CMK-1 taken using JEM-2000FXII (Jeol) operating at 200 kV.

Effect of Cobalt Loading on the Graphitization of Nanoporous Carbon



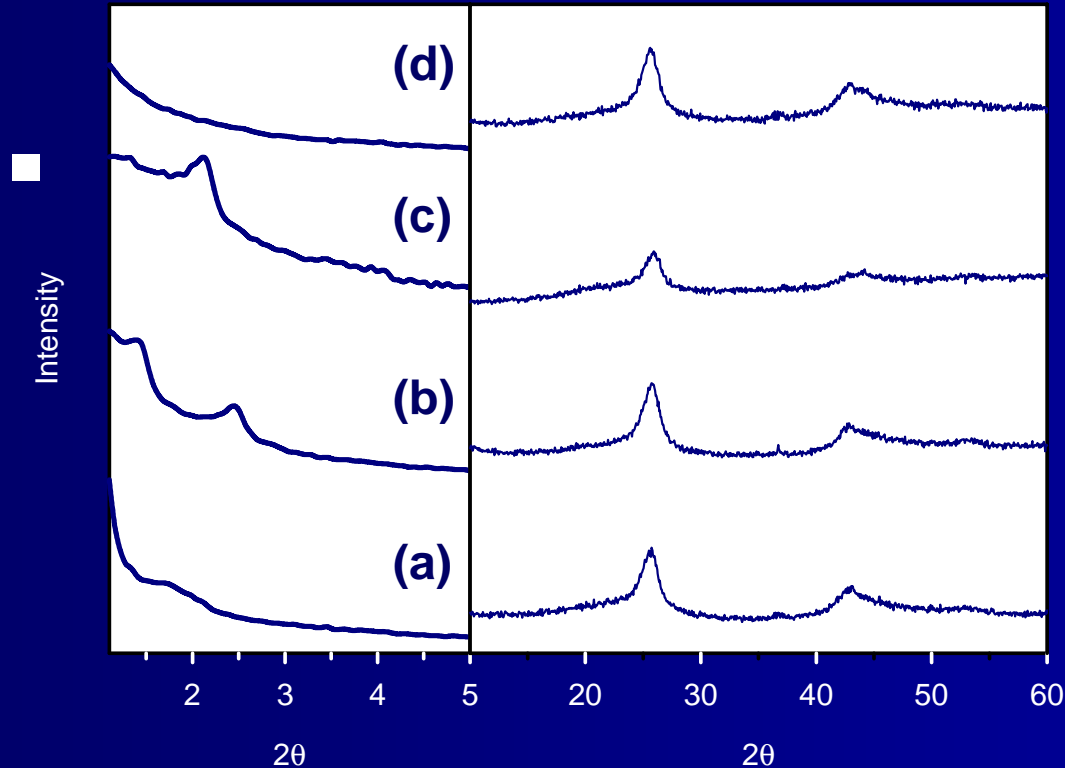
X-ray diffraction patterns of (a) 0 wt%, (b) 2 wt%, (c) 5 wt%, (d) 10 wt%, (e) 15 wt% Co-incorporated nanoporous carbon. The nominal weight percent of Co was based on assuming 60% carbonization yield.

Formation of Nanoporous Carbon from Nanoporous Silica



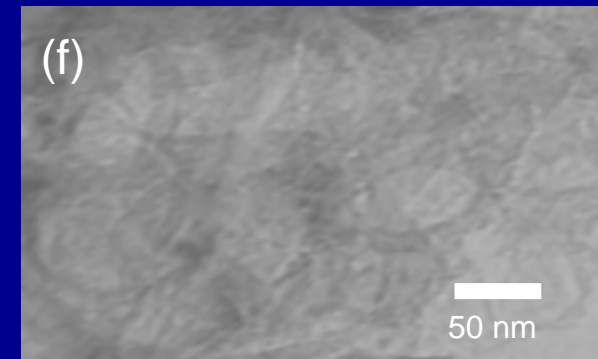
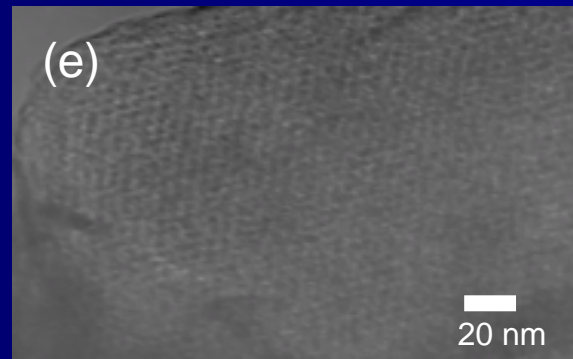
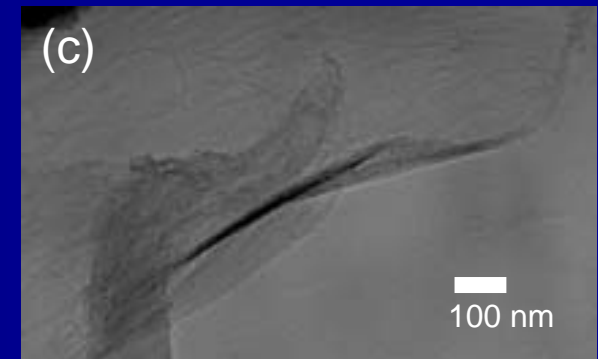
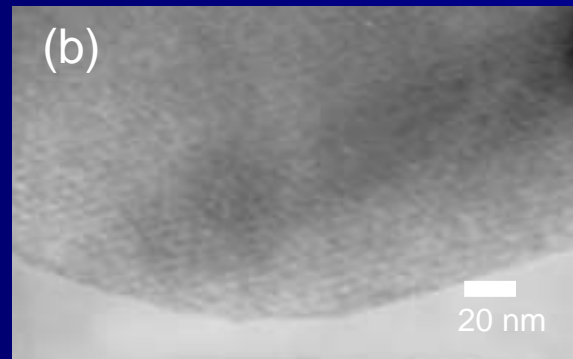
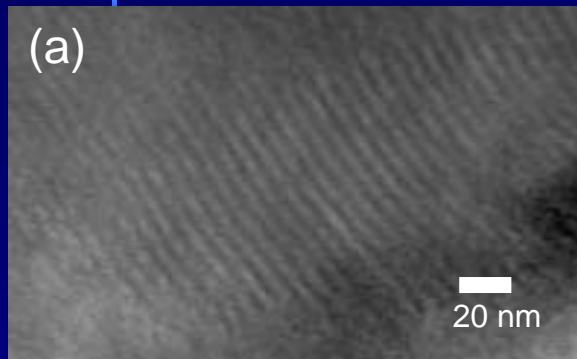
Nanoporous carbon templated with furfuryl alcohol from (a) SBA-15, (b) MCM-48, (c) two dimensional hexagonals and (d) MCM-41.

Formation of Graphitized Nanoporous Carbon from Nanoporous Silica



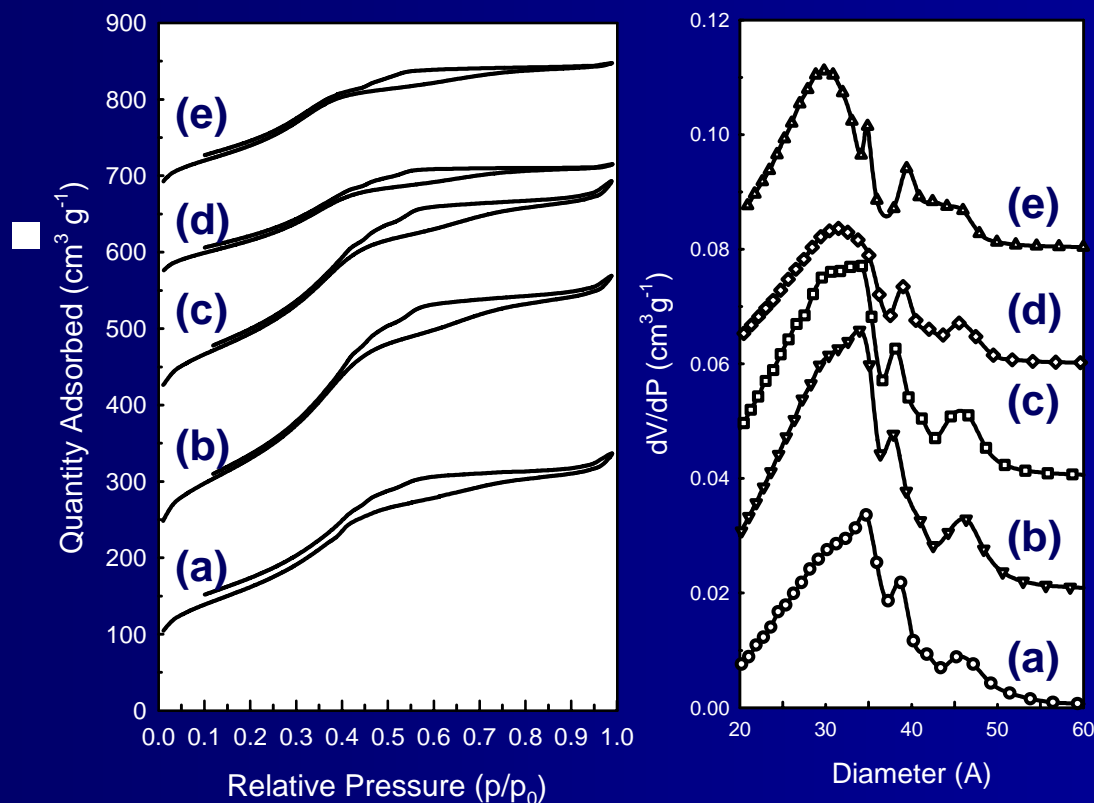
Graphitized Nanoporous carbon templated with furfuryl alcohol from (a) SBA-15, (b) MCM-48, (c) two dimensional hexagonals and (d) MCM-41.

Transmission Electron Micrographs of the Metal Incorporated Nanoporous Carbons



Transmission electron micrographs of the carbon replicas from (a,d) SBA-15, (b,e) two dimensional hexagonal silica's, (c, f) MCM-41. The micrographs of (a), (b) and (c) are without the incorporation of Co and the micrographs of (d), (e) and (f) are with the incorporation of Co into the nanoporous carbons.

N₂ BET Adsorption on Pd Incorporated Carbon at 77 K



N₂ BET adsorption isotherms and pore size distribution of (a) 0 wt%, (b) 1 wt%, (c) 2 wt%, (d) 4 wt%, (e) 8 wt% Pd incorporated nanoporous carbon measured at 77 K using ASAP2020 instrument (Micromeritics)

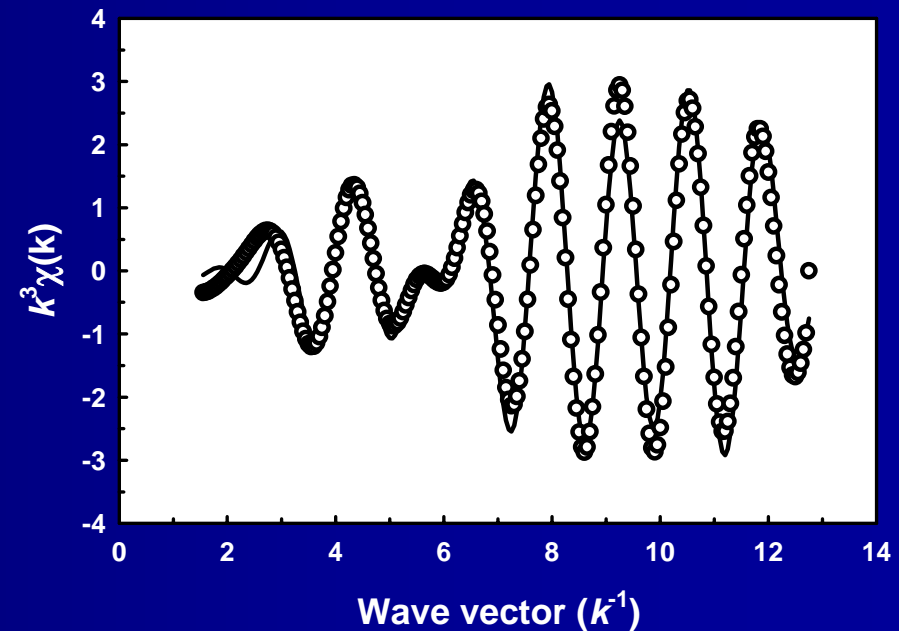
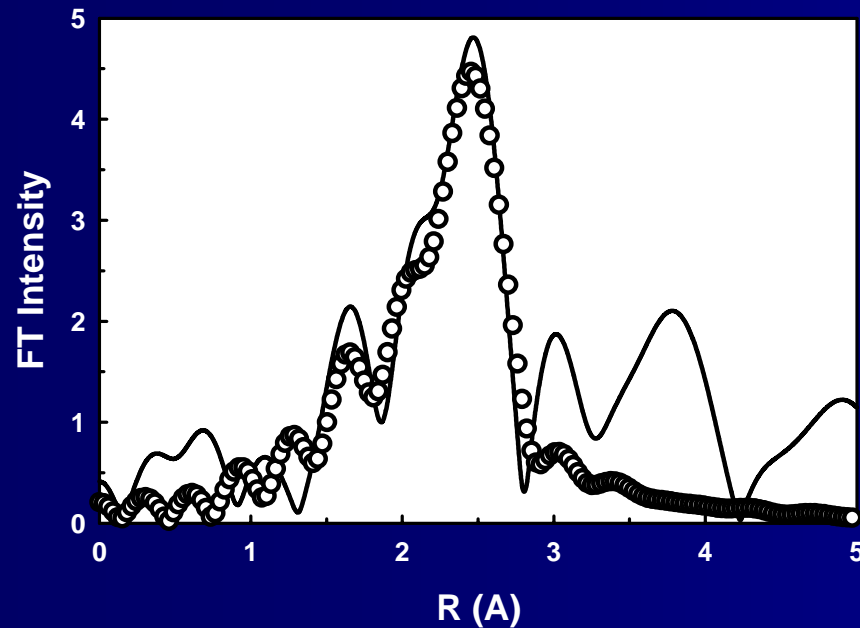
Summary of N₂ BET Adsorption Measurement on Pd Incorporated Carbon

Pd wt%	S _{BET} (cm ² g ⁻¹)	V _p (cm ³ g ⁻¹) ^a
0	581.4	0.565
1 ■	826.1	0.784
2	697.0	0.657
4	414.5	0.374
8	502.4	0.439

^aCalculated from the desorption isotherms between 2-30 nm

Incorporation of Pd into nanoporous carbon did not affect much on the porosity.

Extended X-ray Absorption Fine Structure at Pd K Edge of 8 wt% Pd in Carbon



Pd in the carbon framework showed the Pd-Pd and Pd-C coordination, which indicated **the formation of Pd/PdC nanoparticles.**

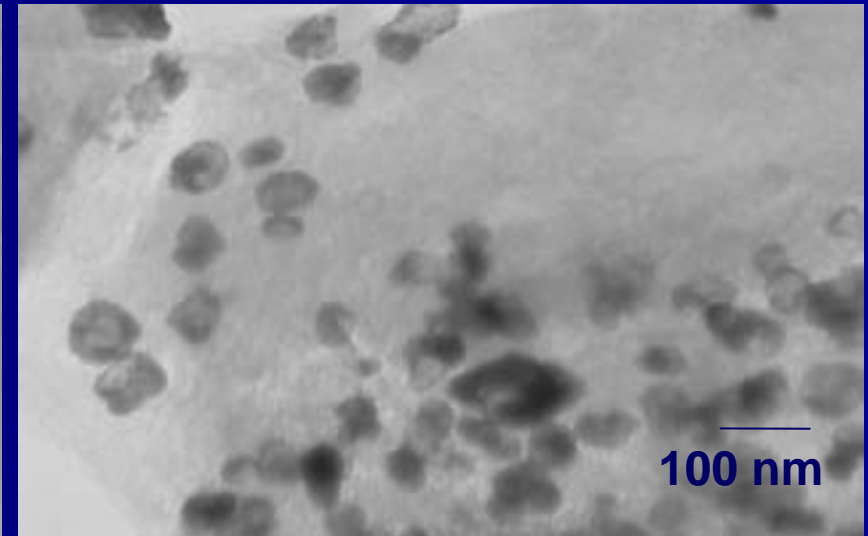
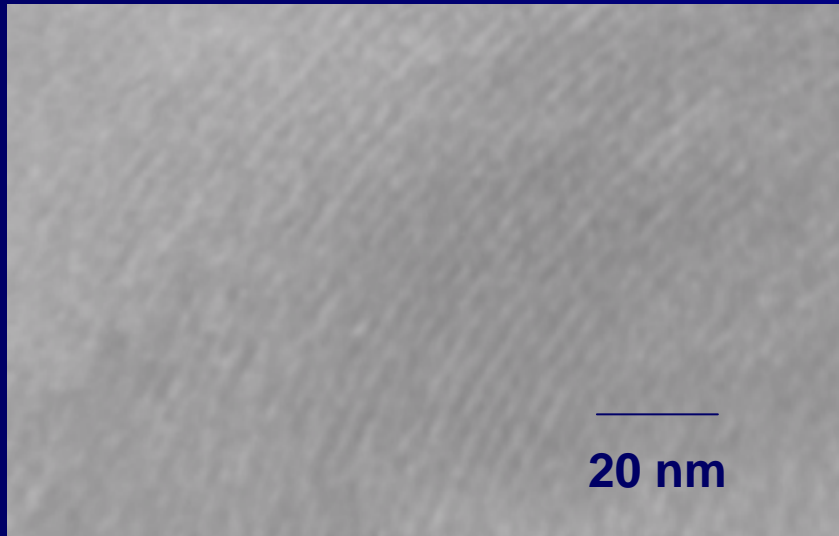
Structural Parameters of Pd Incorporated Nanoporous Carbon from the Curve Fit

Pd wt%	Pair	CN	R	σ^2 (pm ²) ^a
4	Pd-Pd	1.6	2.71	48
	Pd-C	1.6	2.77	-
8	Pd-Pd	1.6	2.75	66
	Pd-C	1.3	2.56	-

^aThe Debye-Waller factor. The many reduction factor was assumed to be 0.9.

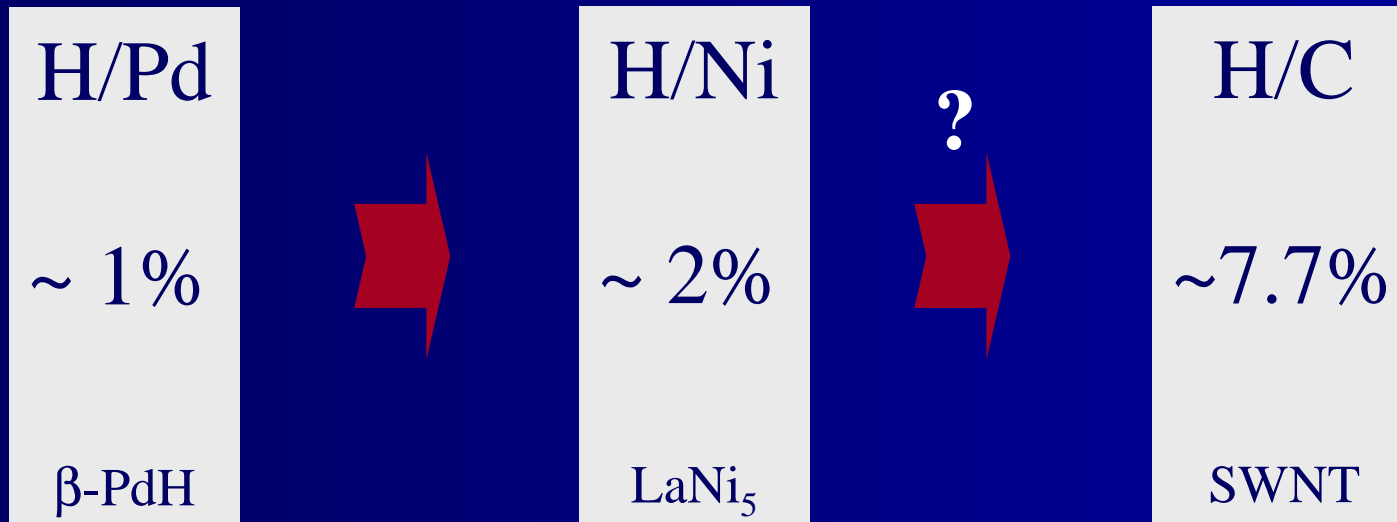
Identification of Pd-C bond was direct evidence for the formation of PdC in the nanoporous carbon framework.

Transmission Electron Micrographs of Pd Incorporated Carbon



Nanoporous carbon showed a nanopore about 3-4 nm. Pd metal particle embodied in the carbon framework was observed but very weak electron diffraction, indicating the formation of PdC composite.

Hydrogen Chemisorption Stoichiometry



Conducting Polymer : New Potential Hydrogen Storage Media

High conductivity of conducting polymers : 100 to 400 S/cm for polyaniline doped with camphor sulfonic acid (PANI-CSA).

(J. Joo et al., *Phys. Rev. B* 57, 9567 (1998))

Metallic natures of PANI-CSA :

[1] Positive temperature coefficient of the resistivity at high temperatures

[2] Linear temperature dependence of thermoelectric power

[3] Frequency independent of conductivities.

(C. O. Yoon et al., *Synthetic Metals* 69, 2250 (1995))

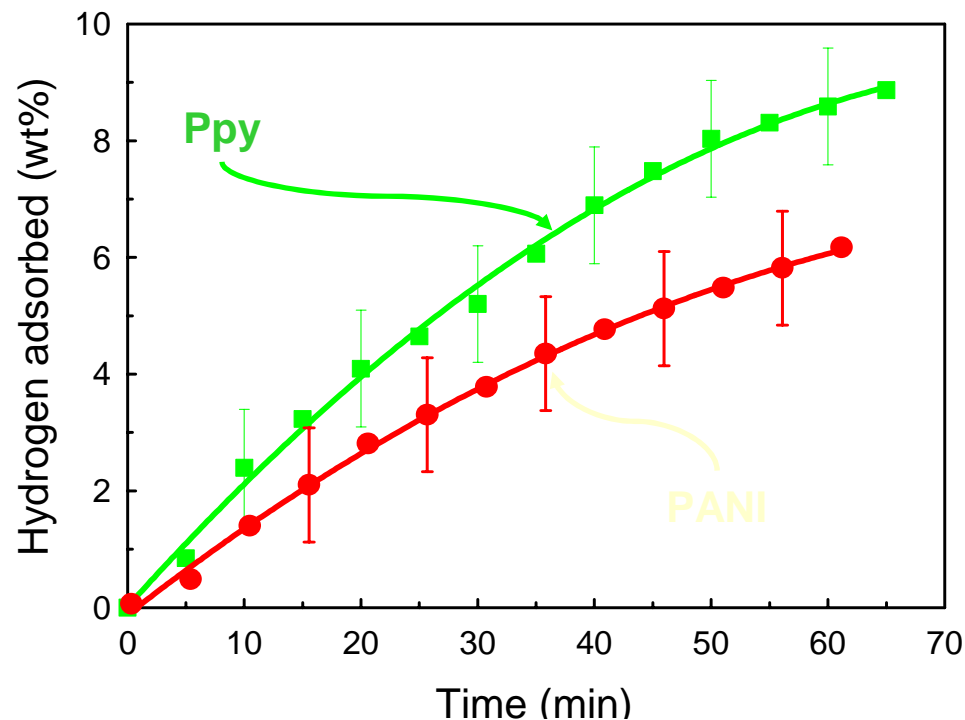
Electron transport properties of organic conducting polymer were found to show remarkably similar behaviors to those of mats consisting of unoriented SWNTs.

(A. B. Kaiser, G. H. Flanagan, D. W. Stewart, D. Beaglehole, *Synthetic Metals* 117, 67 (2001))

Achievable conductivity of PANI-CSA surpasses that of copper if the entire charge carrier density in the localized metallic islands containing delocalized carriers participates in the conduction process.

(J. Joo et al., *Phys. Rev. B* 50, 12226 (1994).)

Hydrogen Adsorption on HCl Treated CP ($P_{ini} \sim 90$ atm)



The amount of H_2 in wt % for both the PANI and the Ppy treated with concentrated hydrochloric acid. The measurement was started after evacuation at 473 K and subsequently at room temperature till at least 0.13 Pa. The amount of hydrogen sorption was calculated based on the pressure change after the calibration with the control data. The control data was measured using the empty cell before and after the change of sample.

Summary of Hydrogen Storage in Reference Materials

Sample	Press. (atm)/Temp. (K)	wt%
MmNi _{4.7} Al _{0.3} (AB ₅ type)	10 ~ 20/298	1.2
MmNi _{4.8} Al _{0.2} (AB ₅ type)	10 ~ 20/298	1.3
Ti _{0.7} Zr _{0.3} Mn _{1.0} Cr _{0.9} Ni _{0.02} Fe _{0.03} (AB ₂ type)	10 ~ 20/298	2.0
Multi-wall carbon nanotube ^{a, b}	90/298	0.8
HCl-treated PANI^b	90/298	6.0
HCl-treated Ppy^b	90/298	8.0

^aSynthesized from the decomposition of CH₄ at 800 ~ 1100 K over the catalysts such as Ni/MgO and Ni/USY. The purification of the obtained CNT was carried out in order to remove amorphous carbon by dissolving the sample in HF solution and then ultrasonicated.

^bexposed to ~ 90 atm ultra high purity hydrogen (99.999%) for one hour.

Challenges in Hydrogen Storage Business

[1] Microporous carbon

- Room temperature and high pressure
- ■ Reproducible results
- Unique adsorption properties

[2] Metal incorporated nanoporous carbon

- Role of metal: activation of hydrogen

[3] Conducting polymer

- Characterization of micropore
- Control of electrical property

Acknowledgement

- Ministry of Science and Technology
- Korea Institute of Science and Technology Evaluation and Planning
- Korea Basic Science Institute (Pusan Branch)
- Korea Institute of Energy Research
- Center for Development of Fine Chemicals, Chonnam National University
- Prof. Gon Seo, Hee Moon, Hyun Yong Lee and Yun Sung Lee at Chonnam National University
- Prof. Ryong Ryoo at KAIST
- Prof. Jaheon Kim at Soongsil University
- Prof. Dong Pyo Kim at Chungnam National University
- Prof. Paolo Ciambelli at Univ. Salerno, Italy
- University of Texas at Dallas, USA
- Korea Carbon Black
- Insilicotech Ltd. Korea
- , Korea